Engineering organic solvent reverse osmosis in hybrid AlO_xH_y / polymer of intrinsic microporosity 1 (PIM-1) membranes using vapor phase infiltration

Yi Ren[a], Benjamin C. Jean[b], Woo Jin Jang[a], Akriti Sarswat[a], Young Joo Lee[a], Emily K. McGuinness[b], Kshitij Dhavala[a], Mark D. Losego[b], Ryan P. Lively*[a]

[a] School of Chemical and Biomolecular Engineering, Georgia Institute of Technology, Atlanta, GA 30332, United States

[b] School of Materials Science and Engineering, Georgia Institute of Technology, Atlanta, GA 30332, United States

Corresponding Author: ryan.lively@chbe.gatech.edu

Abstract

A solvent-free post-treatment process known as vapor phase infiltration (VPI) is used to engineer the organic solvent reverse osmosis (OSRO) performance of polymer of intrinsic microporosity 1 (PIM-1) membranes via infiltration of trimethylaluminum (TMA) metal-organic vapor. The infiltration of inorganic aluminum constituents hybridizes the pure polymer PIM-1 into an organic-inorganic material (AlO_xH_y/PIM-1) with enhanced chemical stability. Due to the reaction-limited infiltration mechanism, homogenous distribution of inorganic loading in PIM-1 is achieved, and the OSRO performance is enhanced. OSRO separations of ethanol/iso-octane mixtures are shown to be capable of breaking the azeotropic composition with a separation factor for ethanol over iso-octane greater than 5 and a permeance of 0.1 $L\,m^{-2}h^{-1}bar^{-1}$. Thus, these organic-inorganic hybrid membranes created via VPI show promise as an alternative method for separating azeotropic liquid mixtures.

Keywords: Organic solvent reverse osmosis, vapor phase infiltration, thin film composite, azeotrope breaking, reaction diffusion transport

1. Introduction

Vapor phase infiltration (VPI) has emerged as a scalable, solvent free post-treatment process that can transform pure polymer products into organic-inorganic hybrid materials with various enhanced properties,[1] including the chemical stability desired for membrane-based organic solvent reverse osmosis (OSRO).[2] During VPI, the polymer membrane is exposed to metal-organic vapors that infiltrate into the polymer. Upon exposure to water, the entrapped metal-organic reacts to form metal oxyhydroxide clusters that are believed to form networks that homogeneously mix with polymer chains on a molecular level. These trapped inorganic species are believed to prohibit the polymer chains from large solvent-induced motions such as swelling or dissolution, preserving the polymer microstructure in organic solvent environments. Since the transformation of pure polymer material to organic-inorganic hybrid material will result in modification of various properties, this technique is receiving increasing attention in the membrane community for multiple purposes, such as hydrophilic modification of polyvinylidene fluoride membranes,[3] tailoring the microporosity of polymer of intrinsic microporosity 1 (PIM-1) for gas pair separation,[4] preserving nanoscale features in polymers during laser induced graphene formation of polyethersulfone,[5] reducing required pyrolysis temperature of CMS fabrication for polyimide of intrinsic microporosity (PIM-PI),[6] improving CO_2 permeation of PIM-1 membrane,[7] and improving chemical stability and separation capabilities of PIM-1 membranes in organic solvent separations.[2]

In this work, the transport dynamics of trimethylaluminum (TMA) infiltration into PIM-1 is studied first. TMA is chosen since it has the highest reactivity and inorganic loading in PIM-1 compared with other commonly used metal-organic precursors, as shown in prior work.[2] Since the infiltration process consists of both TMA diffusion into the bulk PIM-1 and an adduct formation between TMA and the nitrile group in the PIM-1 backbone, the VPI hybridization process could be either diffusion or reaction (adduct formation) limited. After understanding how to properly control the inorganic loading for VPI of AlO_xH_y into PIM-1, the organic solvent reverse osmosis (OSRO) performance of VPI treated PIM-1 membranes (AlO_xH_y /PIM-1) is tuned to improve the separation of ethanol and iso-octane. The mixture of ethanol/iso-octane is selected due to their representation of the alcohol and alkane family, as well as their importance in biofuels and fossil-based fuels.[8] PIM-1 thin film composite membranes with PIM-1 topcoats and crosslinked porous

Matrimid supports are exposed to TMA for the VPI treatment process under different TMA hold times. By controlling the metal-oxide loading of the AlO_xH_y/PIM-1 membranes, the OSRO performance is engineered for separation productivity (permeance) and separation efficiency (rejection or separation factor). Finally, the AlO_xH_y/PIM-1 membranes are shown to break the azeotropic concentration for ethanol/isooctane (80mol% ethanol /20mol% isooctane),[9] thus providing an alternative method for small organic molecule separation with high energy efficiency.[10-13]

2. Experimental Methods

This work is comprised of the following main experiments: PIM-1 synthesis (S1), PIM-1 thin film composite membrane fabrication (S2), vapor phase infiltration treatment of PIM-1 membranes (S3), organic solvent crossflow permeation of the VPI treated membranes (S4), and material characterization via scanning electron microscopy (SEM) and energy-dispersive x-ray spectroscopy (EDS) (S5). The detailed information of all the experimental procedures can be found in the Supporting Information.

3. Results and discussion

Designing composite membrane structure based on rate-limiting mechanism for TMA infiltration into PIM-1. Figure 1a provides a sketch of the VPI process chamber for TMA infiltration into PIM-1 thin film composite membranes. A temperature controller ensures isothermal VPI operation at 90°C. Nitrogen is used to purge and remove humidity, and a vacuum pump is used to ensure a vacuum level of 60 mTorr before infiltration. During infiltration, the PIM-1 membrane in the VPI chamber is first exposed to TMA vapor and then subsequently to water vapor. Figure 1b shows the four most important fundamental steps of one VPI cycle on a molecular level. The infiltration into the PIM-1 top coat was shown as bidirectional (top and bottom sides), as the porous Matrimid support was assumed to provide negligible mass transport resistance. The VPI process begins with surface sorption of TMA on the PIM-1 topcoat (step 1). The metal-organic precursor TMA will then diffuse into the bulk of the polymer, and some of the TMA will react with the nitrile groups in PIM-1 backbone and form immobilized metal-organic adducts (step 2). The remaining free diffusing TMA solutes are removed using vacuum, after which the metal-organic-loaded membrane is exposed to water vapor. The immobilized TMA metal-organic precursors nucleate and grow into metal-oxyhydroxide networks that percolate

throughout the entire polymer matrix, trapping the polymer chains and hindering any chain motions of the polymer, thus enhancing the chemical stability of the resulting composite material (step 3). To conclude the process, all excess water molecules are pumped out of the membrane via vacuum (step 4). Although direct evidence of metal-oxyhydroxide network formation is challenging to obtain, previous work supports the idea of homogenously mixed metal-oxyhydroxide networks and polymer chains. [2, 14, 15] An investigation of the structure and material property of AlO_xH_y/PIM-1 with a more comprehensive charaterization suite than shown here was conducted in prior work. This includes Fourier-Transform Infrared Spectroscopy (FTIR) to show no strong chemical bond between the metal oxide and polymers, nitrogen physisorption to show a modest loss of Braunauer-Emmett-Teller (BET) surface area as PIM-1 is infiltrated with AlO_xH_y, and water contact angle measurement to show a shift towards increased hydrophilicity, among several other techniques.[2] Importantly, dramatic chemical stability enhancement and swelling suppression after the VPI process has also been observed in prior work for a variety of metal-organic/polymer combinations, including TMA/PIM-1.[2, 14]

Figure 1c illustrates the process for fabricating AlO_xH_y/PIM-1 thin film composite (TFC) membranes. Briefly, Matrimid is blade cast and phase inverted to create an asymmetric porous support, which is then crosslinked using diamine immersion crosslinking chemistry.[16] PIM-1 is coated on top of these supports via spin coating with a 70% success rate. The PIM-1 TFC membranes are then run through the VPI process to create the final organic-inorganic hybrid membranes.

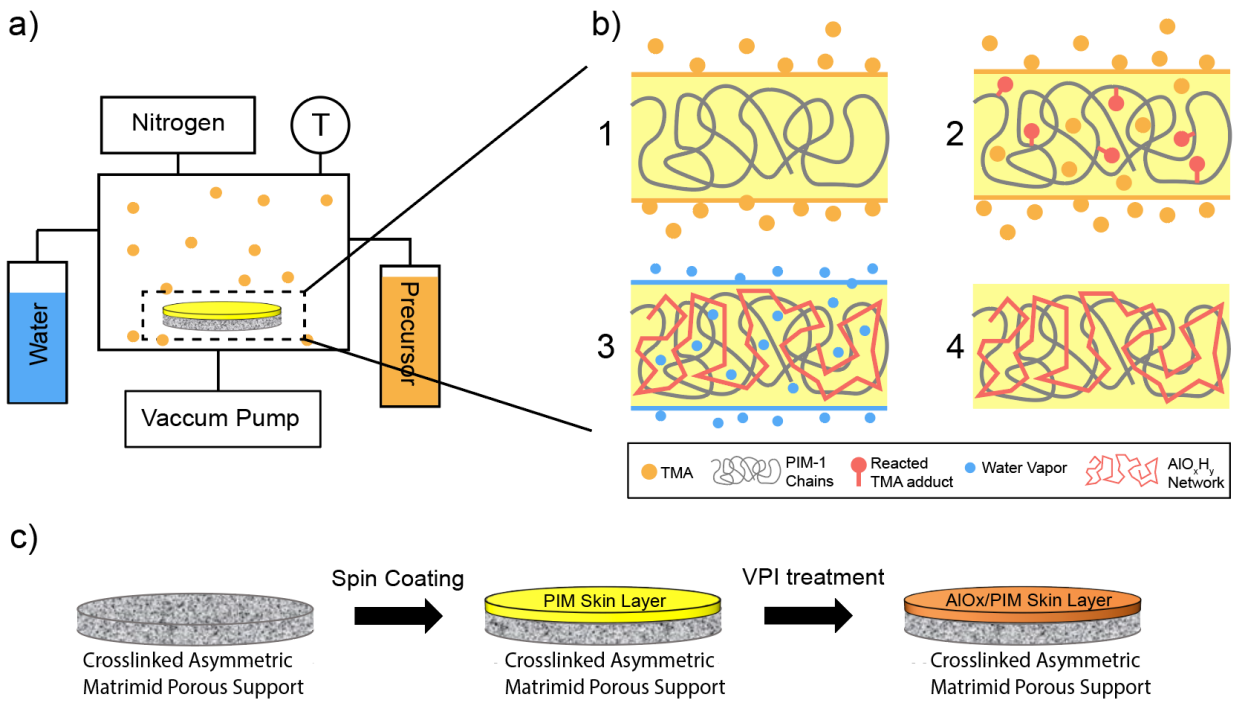

Figure 1. a) VPI reactor set up. b) Schematic of the VPI process into PIM-1 topcoat. c) Fabrication process for VPI-treated PIM-1 thin film composites

The goal of this study is to understand how the quantity of metal oxyhydroxide loading within the PIM-1 TFC affects the membrane's OSRO performance. To achieve this goal, we first designed a series of processes that would create hybrid membranes with varying inorganic compositions by utilizing a reaction-diffusion model for VPI processes that we developed in prior work, and we parameterized the model with information for TMA infiltration into PIM-1 (details provided in S6-S9). Figure 2a and Figure 2b qualitatively illustrates the two common transport mechanisms for VPI metal-organic infiltration processes, which are the reaction-limited case and diffusion-limited case respectively.[17, 18] Both figures describe the different concentration depth profiles of metal-organic loading across the entire thickness of the membrane skin layer as a function of time. Homogenous infiltration of metal-organic loading across the entire thickness of the membrane at short infiltration times can only be achieved in the reaction-limited case due to fast diffusion of the metal-organic precursor and slow reaction. Conversely, Figure 2b illustrates a diffusion-limited case where reaction rate is much faster than diffusion. In this scenario, high surface concentrations can be achieved at early stages due to fast reaction rate, but the bulk of the polymer will not yet be successfully infiltrated due to slow diffusion of the TMA precursor. For

VPI treatment on membranes, reaction limited mechanism represented by Figure 2a is highly desired due to an even distribution of metal-organic loadings across the membrane skin layer, which results in equal degrees of swelling when exposed to organic solvents.

Figure 2c shows the modeled depth profiles for the PIM-1/TMA system as a function of time (from 30 seconds to 20 minutes) for a PIM-1 thin film composite with a 1000 nm thick skin layer, a TMA pressure of 0.8 Torr, and a temperature of 90°C, representing the experimental conditions used in this work (details for obtaining each parameter are in S6-S9). This simulation is based upon bi-direction infiltration of the PIM-1 skin layer, as the porous Matrimid support observed from SEM (Figure 3a) is assumed to provide negligible mass transfer resistance. Due to TMA's high diffusivity in the PIM-1 polymer,[19] this VPI process is expected to be reaction-limited, leading to an even distribution of inorganic concentration throughout the PIM-1 thickness, especially at short TMA exposure times (less than 5 minutes). As the TMA exposure time increases beyond 5 minutes, the inorganic loading in the interior of the membrane increases more slowly with time while the inorganic concentration more rapidly "builds-up" near the surfaces. This "build-up" is indicative of a transition to a diffusion-limited process mechanism caused by a non-Fickian reduction in diffusivity caused by inorganic species adducting to the polymer's functional groups. Thus, while inorganic loading increases uniformly throughout the entire membrane during the first 5 min of VPI, subsequent exposure times are predicted to only increase near-surface concentrations of inorganic. From these predictions, a significant change in OSRO transport performance should be expected over the shorter hold times (30 seconds to 5 minutes) while less dramatic performance changes are expected beyond 5 min of TMA exposure.

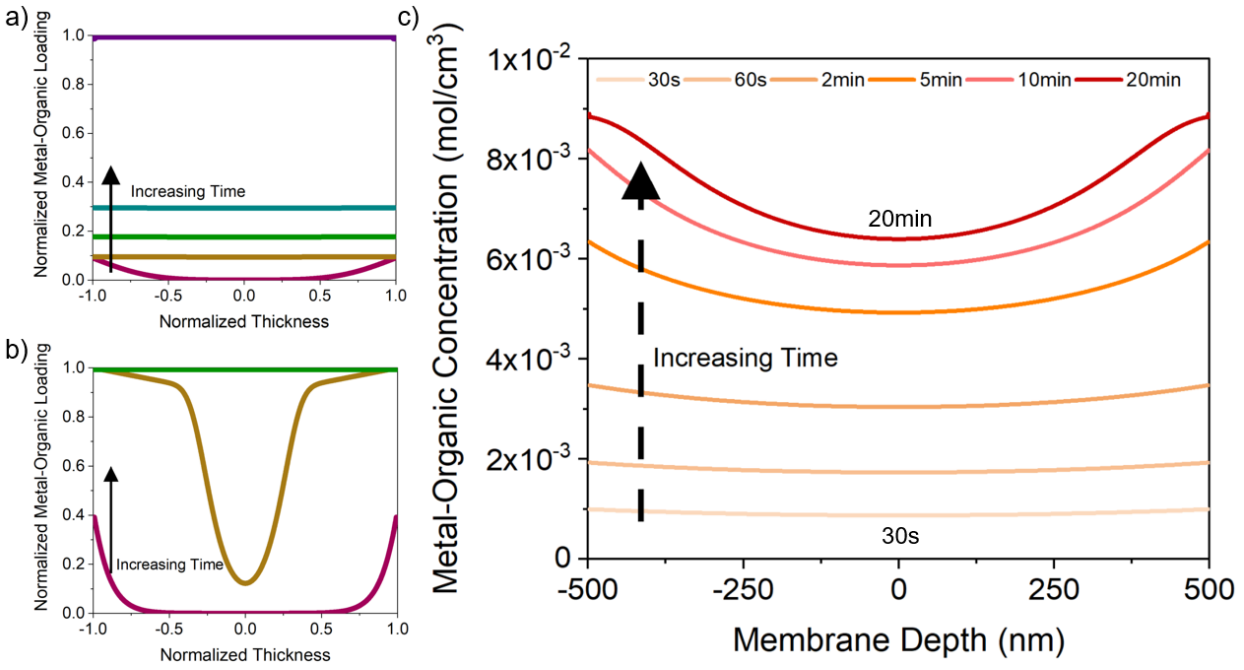

Figure 2. a) Qualitative metal-organic depth profile for reaction-limited VPI scenario. b) Qualitative depth profile for diffusion-limited VPI scenario. a) and b) are reprinted with permission from {Ren, Y.; McGuinness, E. K.; Huang, C.; Joseph, V. R.; Lively, R. P.; Losego, M. D., Reaction–Diffusion Transport Model to Predict Precursor Uptake and Spatial Distribution in Vapor-Phase Infiltration Processes. *Chemistry of Materials* **2021,** *33* (13), 5210-5222}. Copyright {2021} American Chemical Society c) Modeled metal-organic loading depth profile for TMA into PIM-1 thin film composite skin layer with thickness of 1000nm at 90°C, 0.8 Torr. Legends represent increasing TMA hold time from 30s to 20min.

Engineering OSRO performance of PIM-1 thin film composite. Based on our findings with the parameterized reaction-diffusion model for the TMA/PIM-1 system, we conducted a series of VPI experiments with TMA exposure times ranging from 30 seconds to 20 minutes, as the PIM-1 membrane is expected to be saturated after 20 minutes. Figure 3a shows scanning electron microscopy images of the porous Matrimid support and defect-free PIM-1 skin layer topcoat after the VPI treatment. The magnified image shows the PIM-1 topcoat and the corresponding energy-dispersive X-ray spectroscopy (EDS) elemental mapping of aluminum within the PIM-1 skin layer. We note that the EDS map suggests a uniform distribution of aluminum within the topcoat; however, since the PIM-1 skin layer is less than 1 μm thick, with the additional potential instrumental errors and measurement uncertainty from aluminum SEM stubs

and sample drifting, it was challenging to obtain an accurate quantitative measurement of aluminum distribution across the thin PIM-1 top coat, but qualitatively the distribution appears to be uniform.

To initially probe membrane performance, the membranes were tested against a dilute ethanol/iso-octane solution (99 wt% ethanol) in a crossflow permeation experiment. This ethanol (46 Da) / iso-octane (114 Da) mixture is chosen because these small solvent molecules are representative of polar alcohols and non-polar alkanes. Ethanol is also a major component of biofuels, and iso-octane is a critical component of fossil-based fuels such as gasoline,[8] making this separation of high interest for developing sustainable methods to obtain clean energy products.

Using a custom-built crossflow system,[20] under 40 bar and 26 ml/minute (>13.8 cm/s of cross flow velocity) of feed flow for all membranes, it was observed that by controlling the TMA exposure hold time from 30 seconds to 20 minutes, the OSRO performance of AlO_xH_y/PIM-1 membranes could be successfully tuned. As shown in Figure 3b, as TMA exposure hold time increases from 0 seconds to 20 minutes, the permeance (S10) of the AlO_xH_y/PIM-1 membranes decreases from 0.75 $L\,m^{-2}h^{-1}bar^{-1}$ to 0.22 $L\,m^{-2}h^{-1}bar^{-1}$. We speculate that this permeance loss occurs for two reasons. First, the formation of the metal-oxyhydroxide network suppresses solvent-induced polymer chain motions such as swelling and plasticization, thus reducing permeance. Secondly, the VPI hybridization process results in a decrease in free volume of the polymer due to the formation of immobilized product, thus further reducing permeance. Conversely, these two factors are also responsible for an increase in the rejection of iso-octane (S10) from 0% to 74% as the inorganic loading increases with increasing TMA exposure time.

Interestingly, both rejection and permeance plateau when TMA exposure time exceeds 5 minutes (Figure 3b). This result strongly suggests that the accessible nitrile groups in the PIM-1 backbone are fully saturated under these conditions such that any further TMA exposure is unlikely to further improve OSRO performance. To support this hypothesis, the reaction-diffusion VPI transport model is used to estimate the bulk concentration of inorganics in the AlO_xH_y/PIM-1 skin layer as shown in Figure 3c. The predicted inorganic concentration trend aligns well with the observed rejection rate for different TMA exposure hold times, as inorganic loading reaches its saturation point, rejection also plateaus at its maximum value.

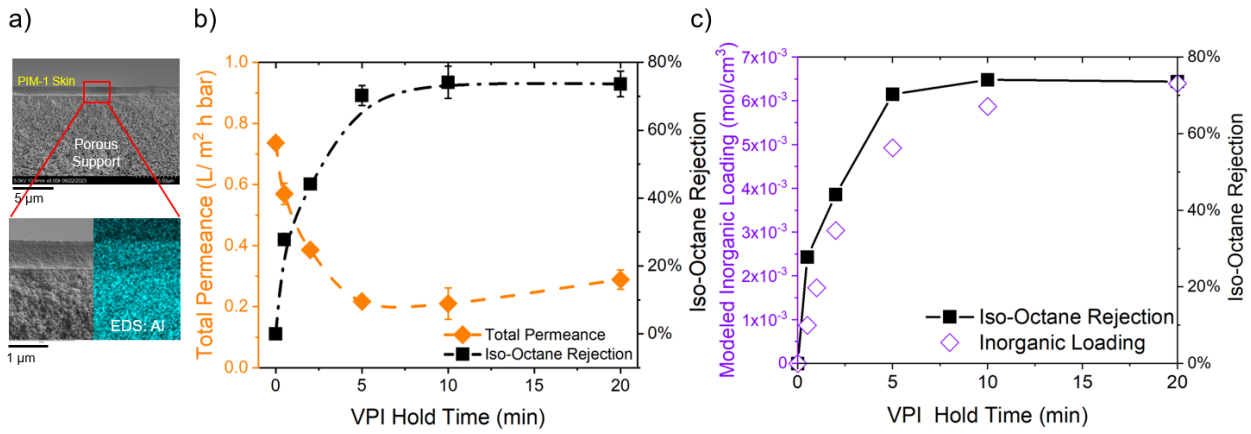

Figure 3. a) Top: Scanning electron micrograph (SEM) of PIM-1 skin layer and porous Matrimid support for PIM-1 thin film composite after VPI treatment. Bottom: EDS elemental mapping of aluminum for AlO_xH_y/PIM-1 thin film composite with 10 min TMA exposure hold time at 90°C and 0.8 Torr. A larger version of SEM image is shown in Figure S1. b) Permeance and rejection of a mixture of 99wt% ethanol, 1wt% isooctane using AlO_xH_y/PIM-1 membranes with different TMA exposure hold times. The custom-built crossflow system was operated under 40 bar, 22°C, and 26 ml/min solvent flow. Error bars are results from 2-4 different membranes in replicates, some error bars are smaller than symbol. c) Comparison between metal-organic bulk loading predicted by VPI transport model and iso-octane rejection for different TMA exposure hold times.

Azeotrope breaking of ethanol/iso-octane using AlO_xH_y /PIM-1 membranes. Finally, the AlO_xH_y /PIM-1 thin film composite membranes are challenged with the azeotropic composition of 80 mol% ethanol/ 20 mol% iso-octane. These AlO_xH_y /PIM-1 hybrid membranes are compared against Puramem Selective, a commercialized market-leading organic solvent separation membrane from Evonik, and Matrimid 5218, a commonly used polyimide membrane for gas and organic solvent nanofiltration separations. The AlO_xH_y /PIM-1 membrane synthesized via 10 min of TMA hold time, represented by AlO_xH_y /PIM-1_10min was used due to its highest rejection (Figure 3b). Puramem Selective and Matrimid 5218 were also treated with the same VPI process for comparison and are represented as AlO_xH_y / Puramem Selective_10min and AlO_xH_y / Matrimid_10min.

Figure 4 summarizes our results for separating the azeotrope. For clarity, the ethanol/iso-octane separation factor (S10) is reported rather than the rejection rate since ethanol and iso-octane

have comparable mole fractions (80 mol% vs. 20 mol%) and thus, no clear distinction can be made between solvent and solute. Under 40 bar, at an ethanol permeance of 0.092 $L\,m^{-2}h^{-1}bar^{-1}$, AlO_x/PIM-1_10min achieves a separation factor of 3.69 (equivalent to 71.9% rejection). As pressure increases to 60 bar, this separation factor increases further to 5.17+/- 2.16 (76% rejection), with a permeance of 0.1 +/- 0.01 $L\,m^{-2}h^{-1}bar^{-1}$. This condition results in an ethanol purity in the permeate of 96 mol% (Figure 4b), more than sufficient to break the azeotrope for this mixture.

Compared to other commonly used polymer membranes (Fig. 4a), AlO_xH_y /PIM-1_10min has the highest separation factor under both 40 bar and 60 bar operation. Pure PIM-1, with the highest permeance of 0.81 $L\,m^{-2}h^{-1}bar^{-1}$ and 0.72 $L\,m^{-2}h^{-1}bar^{-1}$ under 40 bar and 60 bar respectively, is incapable of molecular separation due to poor chemical stability. Puramem Selective exhibits a reversed trend in rejecting ethanol instead of iso-octane, and worse separation ability with a separation factor of 0.769 and 0.768 for 40 bar and 60 bar, respectively. VPI-treated Puramem Selective has a positive rejection for iso-octane (a separation factor of 1.145) but a low separation factor that may result from defect formation from the vacuum drying of the membrane in the VPI chamber after the Puramem membranes is washed in MeOH to remove polyethylene glycol preservatives. Matrimid, one of the most used polyimide materials for membrane separations,[21, 22] has both lower permeance and separation factor compared to AlO_x/PIM-1_10min. The VPI treatment on the Matrimid membranes does not improve performance, possibly due to the low diffusivity of TMA into the Matrimid 5218 polymer compared to PIM-1 and/or a lack of favorable binding sites.

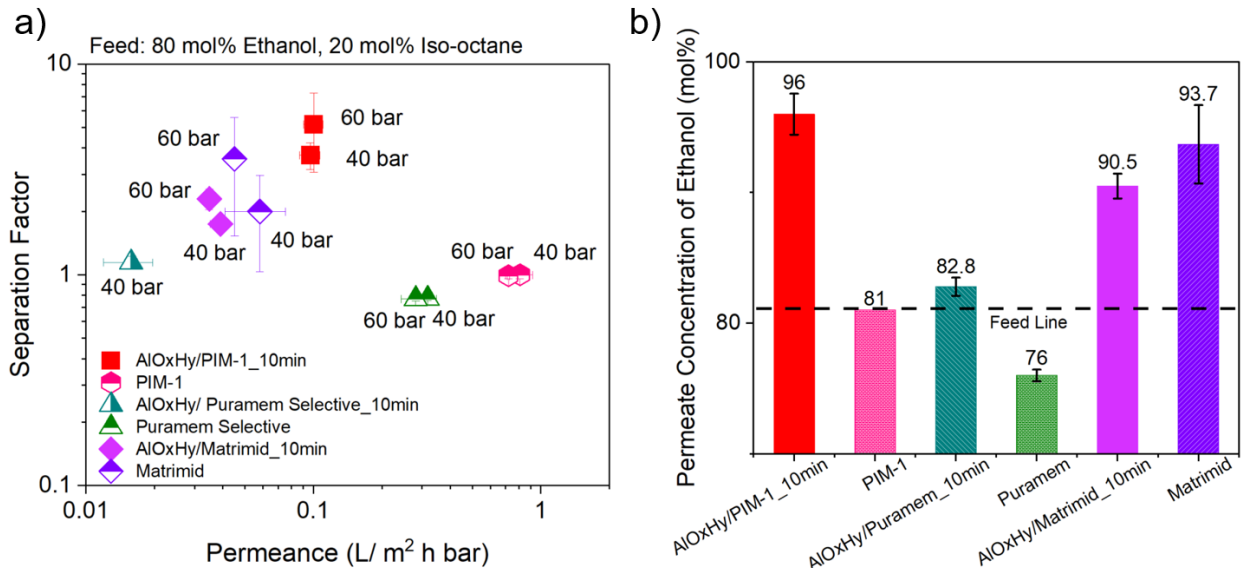

Figure 4. a) AlO_xH_y/PIM-1 membranes with 10 min TMA exposure time compared against other membranes for 80mol% ethanol/ 20mol% iso-octane feed. Crossflow flowrate was 26 ml/min and testing temperature was 22°C. Error bars are results from 2-4 membrane replicates, some errors are smaller than symbol. b) Comparison of ethanol concentration (mol%) in permeate for AlO_xH_y/PIM-1_10min against other standard membranes under 60 bar (except for AlO_xH_y/Puramem_10min which was at 40bar). Dashed line represents the feed mol% of ethanol, which was 81mol%.

4. Conclusions

Here, a post treatment technique known as vapor phase infiltration is used to successfully create hybrid AlO_xH_y/PIM-1 OSRO membranes with the ability to break an alcohol/alkane azeotrope. Based on a parameterized reaction-diffusion VPI transport model for this system, a reaction-limited VPI process was designed to enable a homogeneous distribution of oxide throughout the PIM-1 network. The permeance and rejection of AlO_xH_y /PIM-1 membranes was successfully varied by controlling the TMA exposure time. An "optimized" AlO_xH_y /PIM-1 membrane was found to maximize iso-octane rejection and break the ethanol/iso-octane azeotrope by increasing the ethanol purity from 81 mol% in the feed to 96 mol% in the permeate, although further optimization may be possible via modifying the inorganic hydration and/or number of infiltration cycles. This work provides a solvent-free and time-efficient post-fabrication method for enhancing a polymer membrane's solvent stability to enable small molecule OSRO separations. Although this work supports the hypothesis that OSRO performance can be engineered via the VPI process, other systems beyond PIM-1/ TMA have yet to be explored and thus the suite of materials currently available is limited. Another limitation of this work is related to the VPI transport model used to guide the post-treatments used here. While the current generation of the VPI transport model results are fairly accurate without the swelling terms for the polymers we consider in this work, we acknowledge that strongly dilating polymers may not be accurately modeled using this approach, as polymer thickness is assumed to be constant in the model. Moreover, the relationship between sorption and diffusion of organic solvents into VPI membranes and the VPI processing parameters is currently unknown. Concentration polarization effects could also play a major role in the separation performance of VPI treated membranes and thus an investigation on

concentration polarization could also be beneficial. Future work will involve investigating the transport mechanism of OSRO in VPI treated membranes, as well as exploring other polymer/metal-organic precursor combination in the hope of taking VPI treated membranes closer to industrially relevant separation applications and provide high energy efficient small molecule separation with lower carbon footprint.

Declaration of Competing Interest

The authors declare that they do not have competing financial interests or personal relationships that could have appeared to influence the work reported in this paper.

Acknowledgements

This work was supported by National Science Foundation (DMREF-1921873). SEM images were supported by Institute for Electronics and Nanotechnology (IEN), a member of the National Nanotechnology Coordinated Infrastructure (NNCI), which was supported by the National Science Foundation (ECCS-2025462). The authors would also like to thank Isaiah Borne and Ronita Mathias for helpful discussions regarding PIM-1 synthesis and spin coating procedure.

References

1. Leng, C. Z.; Losego, M. D., Vapor phase infiltration (VPI) for transforming polymers into organic–inorganic hybrid materials: a critical review of current progress and future challenges. *Materials Horizons* **2017,** *4* (5), 747-771.

2. McGuinness, E. K.; Zhang, F.; Ma, Y.; Lively, R. P.; Losego, M. D., Vapor Phase Infiltration of Metal Oxides into Nanoporous Polymers for Organic Solvent Separation Membranes. *Chemistry of Materials* **2019,** *31* (15), 5509-5518.

3. Li, N.; Zhang, J.; Tian, Y.; Zhang, J.; Zhan, W.; Zhao, J.; Ding, Y.; Zuo, W., Hydrophilic modification of polyvinylidene fluoride membranes by ZnO atomic layer deposition using nitrogen dioxide/diethylzinc functionalization. *Journal of Membrane Science* **2016,** *514*, 241-249.

4. Chen, X.; Wu, L.; Yang, H.; Qin, Y.; Ma, X.; Li, N., Tailoring the Microporosity of Polymers of Intrinsic Microporosity for Advanced Gas Separation by Atomic Layer Deposition. *Angew Chem Int Ed Engl* **2021,** *60* (33), 17875-17880.

5. Bergsman, D. S.; Getachew, B. A.; Cooper, C. B.; Grossman, J. C., Preserving nanoscale features in polymers during laser induced graphene formation using sequential infiltration synthesis. *Nat Commun* **2020,** *11* (1), 3636.

6. Ogieglo, W.; Puspasari, T.; Hota, M. K.; Wehbe, N.; Alshareef, H. N.; Pinnau, I., Nanohybrid thin-film composite carbon molecular sieve membranes. *Materials Today Nano* **2020,** *9*.

7. Niu, X.; Dong, G.; Li, D.; Zhang, Y.; Zhang, Y., Atomic layer deposition modified PIM-1 membranes for improved CO2 separation: A comparative study on the microstructure-performance relationships. *Journal of Membrane Science* **2022,** *664*.

8. Grubel, K.; Chouyyok, W.; Heldebrant, D. J.; Linehan, J. C.; Bays, J. T., Octane-On-Demand: Onboard Separation of Oxygenates from Gasoline. *Energy & Fuels* **2019,** *33* (3), 1869-1881.

9. Bader, A.; Keller, P.; Hasse, C., The influence of non-ideal vapor–liquid equilibrium on the evaporation of ethanol/iso-octane droplets. *International Journal of Heat and Mass Transfer* **2013,** *64*, 547-558.

10. Gin, D. L.; Noble, R. D., Chemistry. Designing the next generation of chemical separation membranes. *Science* **2011,** *332* (6030), 674-6.

11. Marchetti, P.; Jimenez Solomon, M. F.; Szekely, G.; Livingston, A. G., Molecular separation with organic solvent nanofiltration: a critical review. *Chem Rev* **2014,** *114* (21), 10735-806.

12. Rivera, M. P.; Bruno, N. C.; Finn, M. G.; Lively, R. P., Organic solvent reverse osmosis using CuAAC-crosslinked molecularly-mixed composite membranes. *Journal of Membrane Science* **2021,** *638*.

13. Sholl, D. S.; Lively, R. P., Seven chemical separations to change the world. *Nature* **2016,** *532* (7600), 435-7.

14. McGuinness, E. K.; Leng, C. Z.; Losego, M. D., Increased Chemical Stability of Vapor-Phase Infiltrated AlOx–Poly(methyl methacrylate) Hybrid Materials. *ACS Applied Polymer Materials* **2020,** *2* (3), 1335-1344.

15. Liu, Y.; McGuinness, E. K.; Jean, B. C.; Li, Y.; Ren, Y.; Rio, B. G. D.; Lively, R. P.; Losego, M. D.; Ramprasad, R., Vapor-Phase Infiltration of Polymer of Intrinsic Microporosity 1

(PIM-1) with Trimethylaluminum (TMA) and Water: A Combined Computational and Experimental Study. *J Phys Chem B* **2022,** *126* (31), 5920-5930.

16. Lee, Y. J.; Chen, L.; Nistane, J.; Jang, H. Y.; Weber, D. J.; Scott, J. K.; Rangnekar, N. D.; Marshall, B. D.; Li, W.; Johnson, J. R.; Bruno, N. C.; Finn, M. G.; Ramprasad, R.; Lively, R. P., Data-driven predictions of complex organic mixture permeation in polymer membranes. *Nat Commun* **2023,** *14* (1), 4931.

17. Ren, Y.; McGuinness, E. K.; Huang, C.; Joseph, V. R.; Lively, R. P.; Losego, M. D., Reaction–Diffusion Transport Model to Predict Precursor Uptake and Spatial Distribution in Vapor-Phase Infiltration Processes. *Chemistry of Materials* **2021,** *33* (13), 5210-5222.

18. Balogun, S. A.; Ren, Y.; Lively, R. P.; Losego, M. D., Interpreting inorganic compositional depth profiles to understand the rate-limiting step in vapor phase infiltration processes. *Phys Chem Chem Phys* **2023,** *25* (20), 14064-14073.

19. Budd, P. M.; Elabas, E. S.; Ghanem, B. S.; Makhseed, S.; McKeown, N. B.; Msayib, K. J.; Tattershall, C. E.; Wang, D., Solution-Processed, Organophilic Membrane Derived from a Polymer of Intrinsic Microporosity. *Advanced Materials* **2004,** *16* (5), 456-459.

20. Thompson, K. A.; Mathias, R.; Kim, D.; Kim, J.; Rangnekar, N.; Johnson, J. R.; Hoy, S. J.; Bechis, I.; Tarzia, A.; Jelfs, K. E.; McCool, B. A.; Livingston, A. G.; Lively, R. P.; Finn, M. G., N-Aryl-linked spirocyclic polymers for membrane separations of complex hydrocarbon mixtures. *Science* **2020,** *369* (6501), 310-315.

21. Soroko, I.; Lopes, M. P.; Livingston, A., The effect of membrane formation parameters on performance of polyimide membranes for organic solvent nanofiltration (OSN): Part A. Effect of polymer/solvent/non-solvent system choice. *Journal of Membrane Science* **2011,** *381* (1-2), 152-162.

22. Lee, J. S.; Adams, R. T.; Madden, W.; Koros, W. J., Toluene and n-heptane sorption in Matrimid® asymmetric hollow fiber membranes. *Polymer* **2009,** *50* (25), 6049-6056.